www.czasopisma.pan.pl PAN POLSKA AKADEMIA NAUK www.journals.pan.pl

Arch. Metall. Mater., Vol. 61 (2016), No 1, p. 411–418

DOI: 10.1515/amm-2016-0075

A.J. DOLATA*,#

CENTRIFUGAL INFILTRATION OF POROUS CERAMIC PREFORMS BY THE LIQUID Al ALLOY – THEORETICAL BACKGROUND AND EXPERIMENTAL VERIFICATION

The goal of this work is the description of phenomena occurring during centrifugal infiltration of porous ceramic materials by liquid Al alloy. In this method, the pressure required to infiltration of liquid metal into pores of ceramic is generated by centrifugal force. From the beginning it was assumed that the porous ceramic material will create reinforcement layer in specific area of the casting. The forces that influence on the liquid metal during mould centrifugation and heat exchange between ceramic preform and metal alloy within the area of the front of infiltration were considered in the analysis. The paper presents also selected experiment results.

Keywords: aluminium casts, Al_2O_3 porous performs, local reinforcement, centrifugal infiltration.

1. Introduction

For several years the studies conducted in area of metal composites are focused on design and production of new products with inhomogeneity structure and heterogeneous properties, such as functionally graded materials [1,2] and locally reinforced materials [3-7]. It allows on better adaptation of the products properties to their specific working conditions. Various production technologies can be used to obtaining of local reinforcement in selected areas of the casting. It seems that infiltration methods are most effective and versatile because they can be used for different metal alloys and various types and forms of reinforcement, such as particles, fibres, woven or porous materials.

1.1. Porous ceramic materials

Porous ceramic materials have many advantageous properties, both the physical and chemical ones (i.e.: low density, high melting point, corrosion resistance, low thermal conductivity, damped vibration capacity). These properties are in close correlation with the structure of porous materials, which is described by specified geometric parameters. The most important are porosity (including the volume fraction of open and closed pores) as well as size distribution and morphology of pores. On the other hand, all the microstructural features depend closely on the selected route of manufacturing porous materials [8-13].

The processing methods used for the preparation of porous ceramic structures such as: foams, honeycomb, interconnected rods, and hollow spheres, were described in detail by Colombo [8]. In turn, relationships between processing - microstructure - property have been reviewed by Studart et al. [8]. Generally, the macroporous ceramic foams (i.e. SiC, Al_2O_3) with porosity in the range from 20% to 97% are produced usually by means of sintering granular materials with expanding agent [10], replication of polymer sponge [11], different direct foaming methods [12] and gel casting of foams [13].

A number of works that are currently in progress focus on the development of method for manufacturing porous ceramic materials intended for semi-finished products that could form the skeleton for infiltration with liquid metal alloys.

1.2. Infiltration processes

Based on the force requirements for infiltration, this technique can be classified into two types: pressureless infiltration (zero force, required wetting the substrate by liquid metal) and pressure-assisted infiltration (external force required). In the literature one can find many articles describing different pressure infiltration processes (PIP) as the most important techniques used for making near-net shape composite products. In such processes, the liquid metal or its alloy under an applied pressure is injected and solidified in a mould packed with preform. Typical examples are: squeeze casting infiltration [6,14,15] and gas pressure infiltration (GPI) [16-20]. The additional pressure may also be generated by the centrifugal force during centrifugal infiltration [5,21-25].

The review of literature indicates a large number of publications in which various pressure-assisted infiltration processes used for making composites based on aluminium matrix and its alloys are described. The available studies describe the structure and properties as well as model assumptions. In the vast majority of cases, they concern metal infiltration into granular [6,25] or fibrous preforms [14-16]. As it results from the review of literature, there are few works on modelling [20] as well as designing the structure and properties of composites

* SILESIAN UNIVERSITY OF TECHNOLOGY, FACULTY OF MATERIALS ENGINEERING AND METALLURGY, KRASINSKIEGO 8, 40-019 KATOWICE, POLAND

Corresponding author: anna.dolata@polsl.pl

obtained as a result of metal infiltration into porous ceramic foam [26-29].

In present work describes of phenomena occurring during centrifugal infiltration of porous ceramic materials by liquid aluminium alloy. In this process, the pressure required to infiltration of liquid metal into pores of ceramic is generated by centrifugal force. From the beginning it was assumed that the porous ceramic material will create reinforcement layer in specific area of the castings.

2. Model studies

The phenomena occurring in centrifugal infiltration of porous ceramic materials with liquid aluminium alloy were analysed taking into consideration the forces that affect liquid metal during mould centrifugation. Heat exchange between preform and metal within the area of the front of infiltration was also considered in the analysis.

2.1. Analysis of forces affecting liquid metal during infiltration

The following analysis assumes that the set of components of forces affecting liquid metal during preform infiltration varies from stage to stage of the process. In this analysis, the infiltration process was divided into four stages.

At the initial stage of the mould casting process, when the air bubble has not been closed in the preform yet (Fig. 1), the liquid metal is affected by: hydrostatic pressure due to rotary motion of the mould, capillary pressure as an effect of conditions under which the ceramic preform is wetted with liquid metal, and resistance of metal flow through porous structure described by Darcy's law.

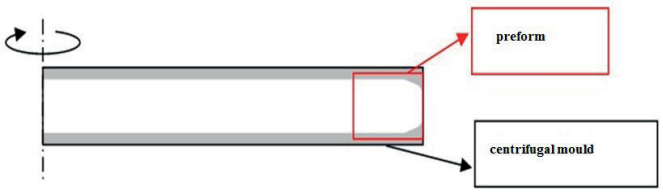

Fig. 1. Stage I – preliminary stage of casting the centrifugal mould

The rotary motion of the mould generates density field of the centrifugal force that affects liquid metal. In simplified single-dimensional model, the centrifugal force direction is in compliance with the mould rotation direction and its value depends on angular velocity ω and distance x from the axis of mould rotation (1).

$$f = \rho\omega^2 x \tag{1}$$

where: ρ- density, ω- angular velocity, x- distance from the axis of mould rotation.

The equation describing hydrostatic pressure (at the bottom of the mould) for given length of the mould L and head of metal poured into the mould H can be derived by integrating the expression (1) over the distance x

$$p_h = \frac{1}{2}\rho\omega^2(2LH - H^2) \tag{2}$$

The capillary pressure counteracting the infiltration of ceramic preform by liquid metal can be determined from expression (3):

$$p_c = \frac{4\gamma\cos(\alpha)}{d_h} \tag{3}$$

where: γ- surface tension, α- wetting angle, d_h- equivalent diameter of pores, equal to the diameter of the reduction of area at links between pores.

The metal flow resistance can be determined based on Hagen-Poiseuille equation:

$$p_d = \frac{28.5}{d_a^{\,2}}\eta v D \tag{4}$$

where: D- depth of infiltration, d_a – equivalent hydraulic diameter of capillaries, η – absolute viscosity of liquid metal, ν- infiltration rate.

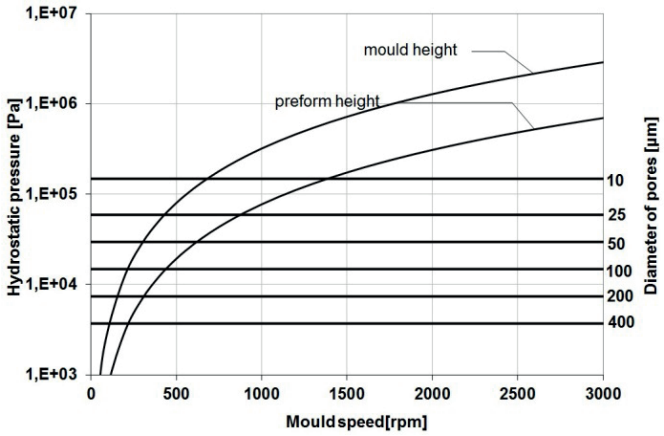

Fig. 2. Capillary pressure vs. hydrostatic pressure obtained for complete mould filling and for filling equal to the height of preform

Fig. 2 presents the summary of capillary pressure with hydrostatic pressure obtained, for different rotational speeds, for ceramic preform (Al_2O_3) with various equivalent capillary diameters. As it can been seen from the diagram, the obtained hydrostatic pressure at the bottom of the mould is enough to overcome the resistance of capillary pressure for the equivalent diameter of pores equal to 10 µm already for the rotational speed of 1500 rpm and the head of metal poured into preform equal to the height of preform.

Fig. 3 presents the summary of hydrostatic pressure with maximum pressure drop (for penetration depth equal to the preform radius) resulting from the resistance of metal flow through porous structure for different rates of infiltration. The head of metal equal to the height of preform was assumed. The analysis of the diagram enables to notice that even for very small equivalent diameters of capillaries (of the order of 10µm), which do not occur in the tested type of preforms, the rotational speed of 2000 rpm allows obtaining the rate of infiltration of the order of 0.2 m/s already at the final depth of preform filling (14.5 mm). The obtained results indicate

that for the adopted rotational speeds of the mould both the capillary pressure and the resistance of flow through porous medium should not be a barrier to preform infiltration by liquid metal.

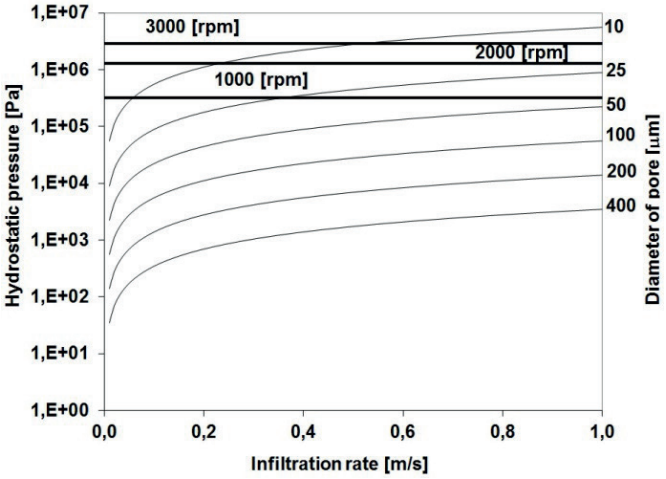

Fig. 3. Summary of pressure drop due to metal flow through porous structure of preform with hydrostatic pressures obtained for various rotational speeds of the mould

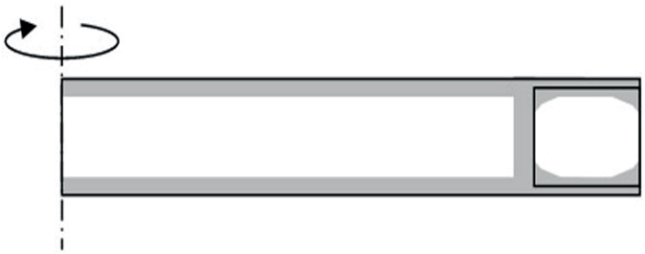

Fig. 4. Stage II – closure of air bubble

Upon the layer of liquid metal has closed the air bubble in the structure of capillary (Fig. 4) the pressure of air compressed in the bubble occurs in the balance of pressures, which must overcome the hydrostatic pressure obtained as a result of rotational motion of the mould. By considering air as a perfect gas and neglecting heat transport between liquid metal and bubble due to the rate of mould infiltration, the resistance of compressed gas can be determined from the following equation (5):

$$p_a = p \cdot \frac{V_{pref}^{\ K}}{\left(V_{pref} - V_{fill}\right)^K} = \frac{p}{\left(1-s\right)^K} \qquad (5)$$

where: p_a – compressed air pressure, p –ambient pressure, s – degree of mould filling, V_{pref} - volume of pores in the preform, V_{fill} - volume of infiltrated metal, K – adiabatic exponent, for air 7/5.

Fig. 5 presents the effect of mould filling, and thus the compression degree of the air entrapped in the bubble, on air pressure counteracting the infiltration of ceramic preform. As it can be seen, at rotational speeds of the order of 3000 rpm the preform filling degree of almost 90% a tenfold compression of the bubble can be obtained.

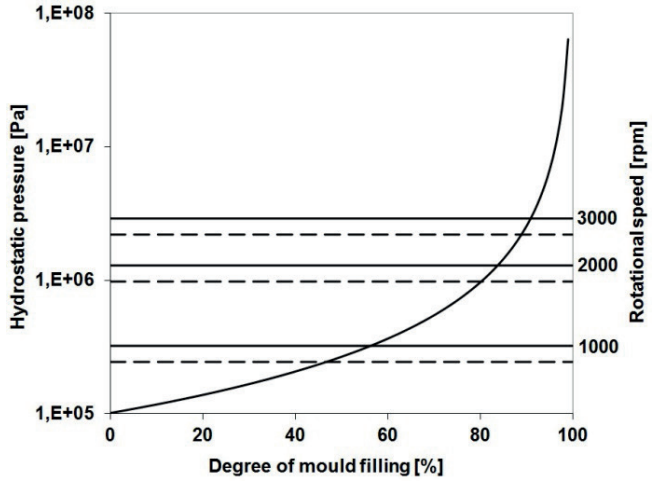

Fig. 5. Resistance of compressed air compared to hydrostatic pressures

When capillary pressure and compressed gas pressure counteract the thrust of hydrostatic pressure, stage III of the infiltration process starts, i.e. movement of gas bubble towards the axis of mould rotation due to the existence of pressure gradient in the preform, Fig. 6.

Fig. 6. Stage III – bubble compression inside preform; ← indicates the direction of capillary pressure

The force affecting the air bubble, which is an effect of difference in pressures on the side closer to the axis of rotation and on the side closer to the bottom of the mould, is proportional to the size of this bubble towards the axis of rotation. The value of this force decreases as the gas bubble approaches the axis, as the gradient is linearly dependent on the distance from the axis of rotation. However, at the same time the size of the bubble increases due to gas expansion. After all, the eightfold increase in volume of the bubble means approximately only twofold increase in its size in direction towards the axis of the mould, which is essential for the difference of hydrostatic pressures that affects it. The braking force of the bubble movement is the force of flow resistance of liquid metal pushed out by it towards the axis of rotation and metal that follows it. As directions of capillary pressure on both sides of the bubble are opposite, its action is counterbalanced and does not affect the bubble movement. However, the elimination of capillary pressure at this stage means that there are no forces that could completely block the movement of the bubble. The above-mentioned flow resistance forces are linearly dependent on speed and thus they only affect the speed of the bubble.

In the last stage IV of the process (with assumption that Al alloy is in the liquid phase), when the air bubble reaches the boundary of the preform, the capillary pressure on the side

closer to the axis of rotation of the mould that counterbalances the capillary pressure on the opposite side decays, Fig. 7.

Fig. 7 Stage IV – pushing the bubble out of the preform; ← indicates the direction of capillary pressure

Therefore, this pressure must be counterbalanced by the difference in pressures on both sides of the bubble. Fig. 8 presents the diagram of relationship between the difference in pressures and the size of the bubble (in the direction of the axis of the mould) lying at the boundary of the preform. As it can be seen from the diagram, the rotational speed of the order of 3000 rpm allows bubbles of 1 mm to be pushed out of a preform with capillaries of the order of 25μm. In case of preforms with bigger size of pores, the difference in hydrostatic pressures, which is the effect of centrifugal force, allows much smaller bubbles to be pushed out of the area of preform.

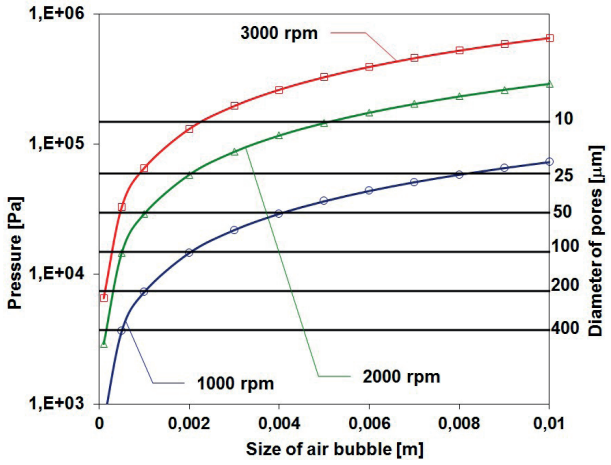

Fig. 8. Changes of pressures as a function of the bubble size

2.2. Heat balance within the area of the infiltration front

In case of ceramic preforms that are usually characterised by higher thermal capacity than the infiltrating metal, crucial for fabrication of composite castings is heat exchange between preform and metal within the area of the infiltration front. Low thermal conductivity of infiltrated and non-infiltrated preform (due to the high volume fraction of low conductive ceramic) causes that heat delivered form metal side by way of thermal conductivity in the case of the analyzed fast infiltration process can be neglected in heat balance of the infiltration front. The temperature of metal and at the same time the volume of solid phase can be determined from the energy balance, which assumes the immediate accomplishment of the state of equilibrium (6):

$$T = \frac{(1-\varepsilon_t)\rho_p c_p T_p + (\varepsilon_t - \varepsilon_e)\rho_g c_g T_p + \varepsilon_e \rho_m c_m T_m + \varepsilon_e \rho_m H_m f(T)}{(1-\varepsilon_t)\rho_p c_p + (\varepsilon_t - \varepsilon_e)\rho_g c_g + \varepsilon_e \rho_m c_m} \quad (6)$$

where: ε_t – total porosity; ε_e – open porosity; ρ_p – density of preform material, c_p – specific heat of preform, T_p – initial temperature of preform, ρ_g – air density, c_g – specific heat of air, ρ_m - metal density, c_m – specific heat of metal, T_m – metal pouring temperature, H_m – heat of fusion, $f(T)$- volume of the solid phase.

The specific air capacity in the equation (6) is dependent on the pressure but the term can be neglected due to its very low value.

The volume of the solid phase is expressed by the following formula (7):

$$f(T) = \begin{cases} 0 & T > T_{liq} \\ \dfrac{T_{liq} - T}{T_{liq} - T_{sol}} & T_{liq} > T > T_{sol} \\ 1 & T_{sol} \end{cases} \quad (7)$$

where: T- metal temperature, T_{lig}- liquidus temperature, T_{sol}- solidus temperature.

The energy balance-based equations used in [14-16] for fibrous preforms do not take into consideration neither the temperature area between liquidus and solidus temperature nor the volume of closed pores, which are not present in this type of preforms.

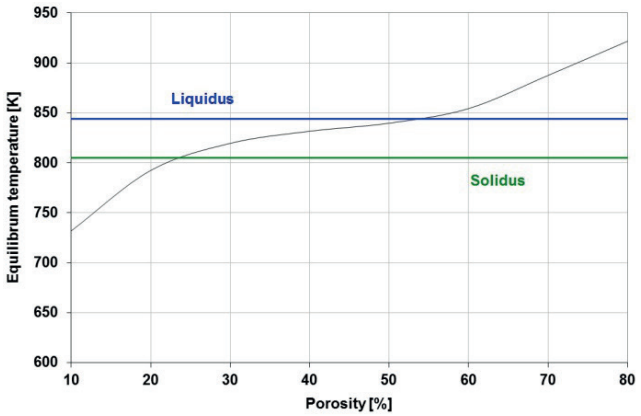

Fig. 9. Dependence of temperature at the front of infiltration on porosity

Fig. 9 presents the dependence of temperature in the area of infiltration front on the porosity for ceramic preform with completely open pores (total porosity equal to effective porosity – no closed pores). The metal casting temperature was assumed to be 993K and the preform temperature – 673K. As it can be seen, below the porosity of 20% there occurs complete metal solidification as a result of heat exchange with preform. Within the porosity range of 20-50%, the equivalent diameter of capillaries decrease as a result of metal solidification (8):

$$d' = \sqrt{1 - f(T)}\, d_a \quad (8)$$

where: $f(T)$- volume of the solid phase, d_a – equivalent hydraulic diameter of capillaries

This way of reduction in capillary diameter will result in increase in the resistance of metal flow through porous structure of the preform expressed by the formula (4).

Fig. 10 presents the dependence of equalisation temperature on changing effective porosity and fixed total porosity equal to 50%. As it can be seen the presence of closed pores in the preform reduces its thermal capacity, and causes that the solidification process starts at the lower open porosity than it has been in the absence of such pores (Fig. 9).

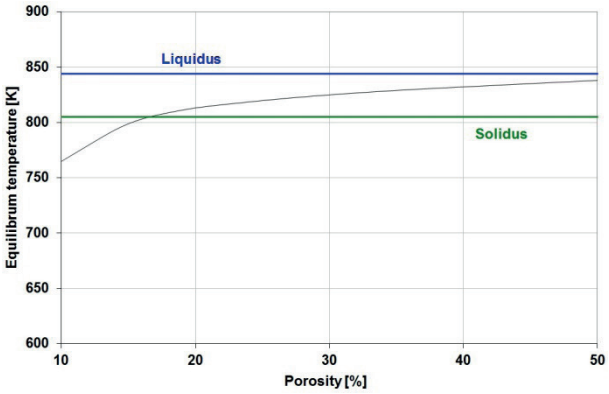

Fig. 10. Dependence of temperature at the front of infiltration on effective porosity, for total porosity of 50%

3. Experiment

In experimental verification of presented simple model two different of porous alumina preforms were used. The preform, which has been prepared by replacement of porous polymer matrix (Al_2O_3_(R)) contained cylindrical pores with different diameter from 100 µm to 600 µm, (Fig. 11a). The total porosity of such porous body was 84%, and the apparent density was 0.60 g/cm^3. The open porosity measured by hydrostatical weight method was equal total porosity (± 1%). In turn, the preform prepared by mechanical foaming and sintering (Al_2O_3_(S)) had pores of irregular shape and their size was within the range from 200 µm to 600 µm, (Fig. 11b). Its total porosity was 50%, (density 2.0 g/cm^3) and contained both open and closed pores. The visible differences in morphology of porous materials (Fig. 11) are resulted from the method used for their fabrication [10].

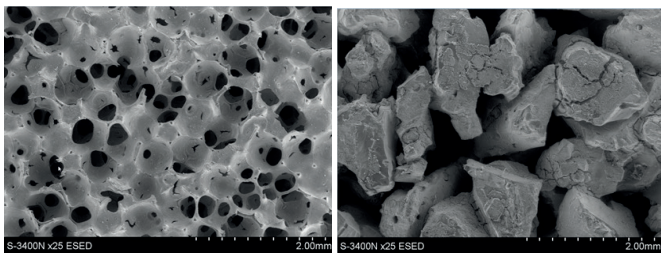

(a) (b)

Fig. 11. SEM micrographs of Al_2O_3 ceramic preforms: a) Al_2O_3_(R) - obtained by replacement of porous polymer matrix with total porosity at a level of 84% and b) Al_2O_3_(S) prepared by sintering of ceramic powder with total porosity at a level of 50%

For infiltration of ceramic preforms EN-AC-AlSi12CuNiMg aluminium alloy modified by 1 wt. % Mg and 0.03 wt. % Sr has been applied. The main process parameters (Tab. 1) were selected on the basis of theoretical analysis. The centrifugal casting equipment and details of infiltration procedures were showed and described in own previous works [5,21-23].

TABLE 1
The main parameters of the centrifugal infiltration

Parameters	Value	Unit
rotational speed of centrifugal mold	4000	rpm
metal casting temperature	993	K
ceramic preform temperature	673	K
pouring time	3	sec

4. Results and discussions

The images of longitudinal section of composite shafts obtained by centrifugal infiltration of aluminium alloy into two different porous Al_2O_3 preforms are shown in Figs. 12 and 13. Due to open cell structure of the Al_2O_3_(R) foams, pores in alumina preform were completely filled by melted aluminium alloy (Fig. 12a). The microstructural analysis of castings in reinforced areas showed lack of defects and structural discontinuities, high degree of pores filling (residual porosity was lower than 1 vol. %) and good connection at the matrix - ceramic boundary. The experimental results and detailed of microstructure investigations, which were widely described in previous works [5,21,23], have confirmed the model assumptions, both the analysis of forces (Fig. 2,3 and Fig. 8) as well as thermal model (Fig. 9) indicate the possibility of full infiltration of the porous preform by the liquid metal alloy.

The result of infiltration test on ceramics fabricated by the mechanical foaming method (open porosity at a level of 20%) is shown in Fig. 13. In this case, quick solidification of metal at the front of infiltration was observed and it prevented from infiltration of the porous ceramic preform by liquid Al alloy. On the basis of the analyzes presented in Figs. 2, 3 and 8, can be concluded that the forces acting on the metal alloy penetrating into the porous preform are not the cause of the lack of infiltration. As shown in Fig. 10 the intensive solidification of liquid metal at the front of infiltration starts if the open porosity is at the level of 20%. In spite of the fact that the metal alloy according to the graph does not achieves the solidus value, but the diameter of the capillary decreases in accordance with equations (7) and (8) at least four times. Additionally, should be taken into account that the real thermal properties and the metal temperature at the start of infiltration may be different from the model assumptions. However, based on the results it can be concluded that the lack of infiltration in the analyzed preforms (Fig. 13) is the result of thermal phenomena.

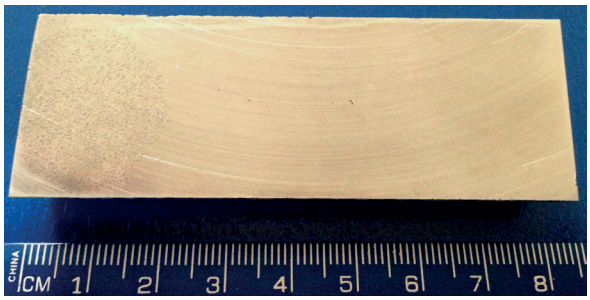

(a)

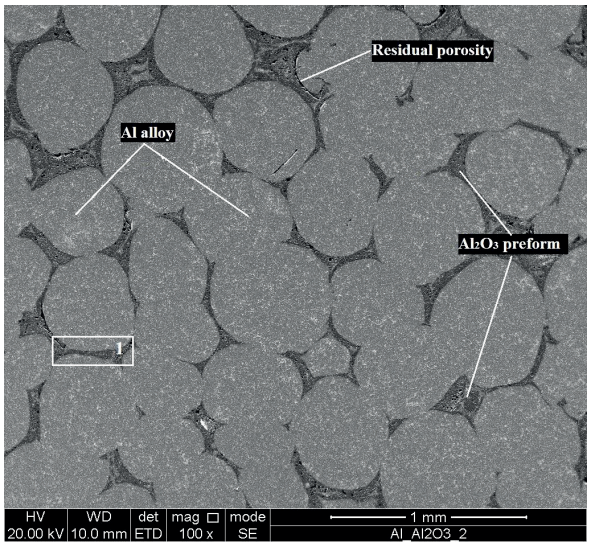

(b)

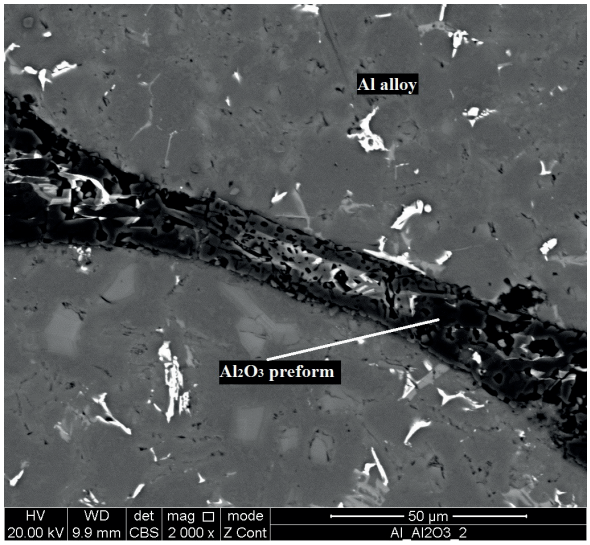

(c)

Fig. 12. Images of a part of casting reinforced locally with Al_2O_3_(R) preform: a) longitudinal section of the half-shaft; b) SEM microstructure within the area of ceramic reinforcement; c) SEM microstructure at a higher magnification within the area marked 1. Bright area is the metal phase; dark area is the ceramic phase.

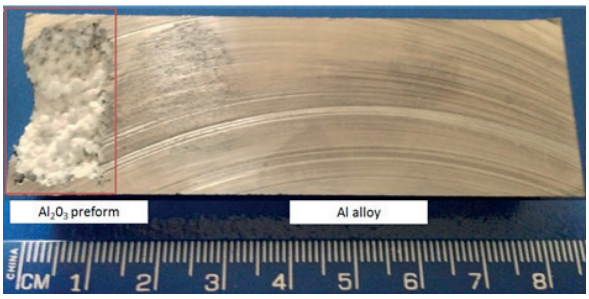

(a)

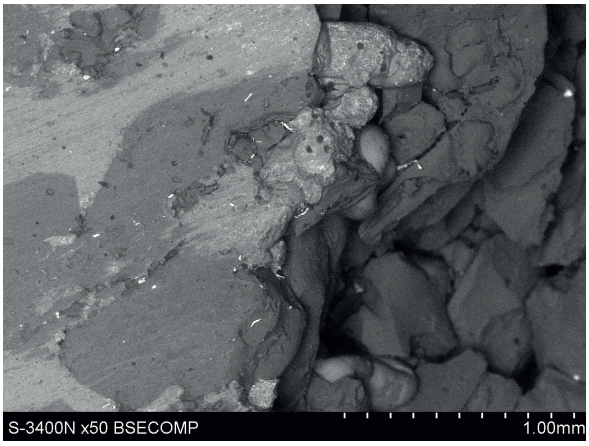

(b)

Fig. 13. Images of a part of casting reinforced locally with Al_2O_3_(S) preform: a) longitudinal section with visible non-infiltrated ceramic preform; b) SEM microstructure in the border area. Bright area is the metal phase; dark area is the ceramic phase

5. Summary

On the basis on results of investigations it has been proved that the centrifugal casting process is effective and may be used for the infiltration of alumina porous preforms by the molten aluminium alloy. The analysis of phenomena occurring during the centrifugal infiltration of porous ceramic structures by the liquid metal required the adjustment of mathematical models described in literature and used for description of the processes of infiltration of fibrous preform [14-16]. The ceramic preforms described in this paper and used in researches were characterised by considerably lower porosity than that of the fibrous preforms, and above all by the existence of closed pores. At the same time, the effectively large size of pores as compared to those of fibrous preforms cause that phenomena such as capillary pressures and flow resistances do not form a significant barrier to the infiltration of preform by the liquid metal. Based on the analysis of results of performed tests, model as well as experimental ones, it has been demonstrated that total and effective porosity of applied ceramic preforms is crucial to the success or failure of the infiltration process. Thus, the method for fabrication of ceramic preforms is of key importance. A property fabricated ceramic skeleton intended for infiltration by liquid metal should be characterised by the structure of linked open pores. Such a structure of ceramic material allows easy penetration of liquid metal into its empty spaces. The occurrence of closed pores may result in formation of micro-voids in the final composite product, and in consequence for decreasing of its properties. Moreover as it

has been demonstrated, for preforms with effective porosity at a level of 20% there occurs the complete metal solidification on preform wall and the infiltration process stops. Therefore the use of ceramics with an open porosity at a level of 20% is not recommended for infiltration process due to the likelihood of the presence of closed pores.

Acknowledgements

The authors would gratefully acknowledge the financial support from National Science Centre in Poland (Project No. N N508 630 540). Furthermore, the experimental works were partially supported within research work performed at the Silesian University of Technology (Project No. BK 220/ RM3/2015).

REFERENCES

[1] J.J. Sobczak, L. Drenchev, J. Mater. Sci. Technol. **29**, (4), 297-316 (2013).
[2] S. Golak, R. Przylucki, IEEE Trans. Magn. **47**, (12), 4701-4706 (2011).
[3] S. Golak, M. Dyzia, J. Mater. Sci. Tech. **31**, (9), 918-922 (2015).
[4] E. Olejnik, S. Sobula, T. Tokarski, G. Sikora, Arch. Metall. Mater. **58**, (3), 769-773 (2013).
[5] A.J. Dolata, Arch. Metall. Mater. **59**, (1), 343-346 (2014).
[6] H.G. Kang, D.L. Zhang, B. Cantor, J. Microsc. **169**, (2), 239-45 (1993).
[7] S. Galak, Adv. Mater. Sci. Eng. **2015**, (Article ID 681939), doi:10.1155/2015/681939 (2015).
[8] P. Colombo, Phil. Trans. R. Soc. **364**, 109-24 (2006).
[9] A.R. Studart, U.T. Gonzenbach, E. Tervoort, L.J. Gauckler, J. Am. Ceram. Soc. **89**, 1771-89 (2006).
[10] A. Oziębło, Z. Jaegermann, S. Traczyk, C. Dziubak, Glass and Ceram. **57**, 1-7 (2006).
[11] M.D.M. Innocentini, P. Sepulveda, V.R. Salvini, V.C. Pandolfelli, J.R. Coury, J. Am. Ceram. Soc. **81**, (12), 3349-52 (1998).
[12] S. Dhara, P.A. Bhargava, J. Am. Ceram. Soc. **86**, (10), 1645-50 (2003).
[13] J.M. Tulliani, M. Lombardi, P. Palmero, M. Fornabaio, L.J. Gibson, J. Eur. Ceram. Soc. **33**, 1567-76 (2013).
[14] T.W. Clyne, J.F., Metall. Trans. A. 18A, 1519-30 (1987).
[15] J.I. Song, Y.C. Yang, K.S. Han, J. Mater. Sci. **31**, (10), 2615-21 (1996).
[16] B. Wang, KM. Pillai, Metall. Mater. Trans. A. **44**, 5834-52 (2013).
[17] A. Mortensen, L.J. Masur, J.A. Cornie, M.C. Flemings, Metall. Trans. A. **20**, 2535-47 (1989).
[18] A. Boczkowska, P. Chabera, A.J. Dolata, M. Dyzia, R. Kozera, A. Oziębło, Solid State Phenomena **191**, 57-66 (2012).
[19] A. Boczkowska, P. Chabera, A.J. Dolata, M. Dyzia, A. Oziębło, Metalurgija **52**, (3), 345-48 (2013).
[20] R. Gil, A. Jinnapat, A.R. Kennedy, Compos. Part. A. **43**, (6), 880-84 (2012).
[21] A.J. Dolata, Solid State Phenomena **212**, 7-10 (2014).
[22] A.J. Dolata, M. Dyzia, in: Proceedings of ICCM-19, Montreal (2013).
[23] A.J. Dolata, J. Mater. Eng. Perform. (2016), DOI: : 10.1007/s11665-016-1901-2 (in press).
[24] M. Sánchez, J. Rams, A. Ureña, Compos. Part A. **41**, 1605-11 (2010).
[25] 2J. Wannasin, M.C. Flemings, J. Mater. Process. Technol. **169**, 143-9 (2005).
[26] H. Chang, J. Binner, R. Higginson, Wear, **268**, 166-71, (2010).
[27] H. Chang, R. Higginson, J. Binner, J. Microsc., **233**, 132-39 (2009).
[28] J. Binner, H. Chang, R. Higginson, J. Eur. Ceram. Soc., **29**, 837-42 (2009).
[29] M. Potoczek, RE. Sliwa, Arch. Metall. Mater. **56**, 29 1265-9 (2011).

Received: 10 March 2015.